9030 *Macromolecules* **2010**, *43*, 9030–9038
DOI: 10.1021/ma101775h

Macromolecules
ARTICLE

# Shear-Induced Nucleation and Growth in Isotactic Polypropylene

**Roberto Pantani,* Ivano Coccorullo, Valentina Volpe, and Giuseppe Titomanlio**

*Department of Chemical and Food Engineering, University of Salerno via Ponte don Melillo, 84084 Fisciano (SA), Italy*

*Received August 3, 2010; Revised Manuscript Received September 25, 2010*

ABSTRACT: The possibility of controlling the final morphology, and thus the resulting mechanical and functional properties, of semicrystalline polymers based on the study of polymer crystallization stimulated by flow is highly intriguing. Recent advances in experimental techniques that allow in situ measurements of material morphology under deformation have escalated research in this subject area. However, despite of the huge efforts spent, the description of the evolution of morphology under shear conditions is still challenging and even the basic principles of the phenomenon are not well understood yet. In this work, experiments of nucleation density and growth rate of spherulites were carried out under continuous shear in a range of temperature (138−144 °C) and shear rate (0−0.30 $s^{-1}$) which, although narrow in absolute, can be considered quite wide taking into account the experimental difficulties presented by this kind of tests. Collected data were analyzed with the aim of determining scaling rules which can describe the effect of flow on crystallization kinetics. It was found that a proportionality exists between nucleation rate and spherulitic growth rate under flow, suggesting that whatever the controlling mechanism for the enhancement of nucleation rate is, it has a similar effect also on growth rate. The effect of flow on nucleation and growth rates was attributed to the increase of the melting temperature due to flow. In turn, the melting temperature estimated for the tests conducted in the whole range of temperatures and shear rates was found to be dependent on the Weissenberg number.

## Introduction

In common polymer processing operations such as injection molding, film blowing, and fiber spinning, the molten polymer is subjected to intense shear and/or elongational flow fields and crystallizes during or after the application of flow. The semicrystalline morphology that develops in the final product is typically very different from what is observed during quiescent crystallization of the same polymer. The high stresses and strain rates experienced by a hot polymer melt as it contacts the cold walls of the die in an injection molding operation can lead to the development of a highly nonuniform "skin-core" morphology. The difference in properties between the highly oriented crystallites in the skin and the spherulitic core can lead to undesirable effects such as stress whitening, warpage, or, in extreme cases, delamination of the skin.[1] On the other hand, a larger skin layer can induce a higher Young's modulus and a larger strain at break.[2]

The possibility of controlling the final morphology and the resulting mechanical and functional properties of semicrystalline polymers[3−17] based on the study of polymer melt crystallization stimulated by flow is highly intriguing. An improved understanding of the fundamentals of flow-enhanced crystallization effects can help to tailor advanced processing strategies which are guided by a better insight into the interplay between macromolecular flow dynamics and polymer crystallization.

Recent advances in experimental techniques that allow in situ measurements of material morphology under deformation have escalated research in this subject area. The recent research has clearly shown that there are qualitatively three regimes of crystallization under shear:[20] (a) very low shear rates, in which there is no effect on kinetics; (b) higher shear rates, in which orientational effects enhance just the nucleation and growth rates, and spherulitic crystallization is observed; and (c) high shear rates, in which molecular stretching occurs giving rise to a fibrillar morphology development under very fast kinetics.

In particular, many of the reported results have been obtained in the intermediate shear rate region, using either rheometrical equipments or commercial shear cells such as for instance the Linkam CSS-450. These studies have clearly demonstrated the enhancement of overall crystallization by effect of the shear flow.[9−17]

A large part of these papers is focused on the nucleation and on the growth rates of spherulites only after the application of the shear flow whereas just a few literature papers deal with the influence of shearing during crystallization. This kind of research is pioneered by Wassner and Maier[18] who qualitatively studied the influence of shearing during isothermal crystallization experiments of iPP by rotation rheometry in combination with optical microscopy coupled with an optical shear cell.

In our previous work,[19] the effect of a steady shear flow applied during crystallization on the morphology evolution and on the kinetics of isothermal crystallization of an iPP was studied experimentally. It was found that nucleation density in quiescent conditions remained constant with time (i.e., no nucleation rate was observed during the test). On the contrary, under shear flow, an increase of nucleation density with time was observed. This increase resulted to be essentially linear with time. The linear dependence allowed to calculate a constant nucleation rate, which was found to be dependent on shear rate according to a power law expression, whose exponent was found to be about 3. During the same tests, it was also possible to collect data of spherulitic radius increase. It was found that the growth rate is essentially constant during the test (both in quiescent and flow conditions), and that it is an increasing function of shear rate. It was found that the effects of flow on the increases of nucleation and growth rates are just proportional to each other.

*Corresponding author.

 Published on Web 10/15/2010 

Despite of the huge efforts spent, the description of the evolution of morphology in shear conditions is thus still challenging. If an understanding of the fundamentals of structure development during processing is sought, additional experimentation of nucleation density and growth rate of spherulites under different temperature and shear rate conditions is required.

In this work, experimentation on nucleation density and growth rate of spherulites were carried out under a wide range of temperature ($T$ = 138−144 °C) and shear rate ($\dot{\gamma}$ = 0−0.30 $s^{-1}$) and data of nucleation density and spherulitic radius were collected during the application of the shear. The range of shear rates is still in the intermediate regime, in which spherulitic crystallization is found.

Collected data were analyzed with the aim of determining scaling rules that can describe the effect of flow on crystallization kinetics.

## Experimental Section

**Material.** In this work, a commercial grade iPP resin (T30G, $M_w$ = 481000, $M_n$ = 75000, tacticity = 87.6%mmmm), kindly supplied by Montell (Ferrara, Italy), was adopted for the experiments. This material is the same as adopted by Titomanlio and co-workers to investigate the effect of a steady shear flow applied during crystallization on the morphology evolution and on the kinetics of isothermal crystallization.[19] In particular, measurements of spherulitic nucleation density and growth rate during isothermal crystallization at a single temperature ($T$ = 140 °C) were carried out under both quiescent and shear conditions (shear rate ranging from 0.07 to 0.30 $s^{-1}$). Moreover, Titomanlio and co-workers adopted this material also to identify a model of crystallization kinetics able to describe morphology evolution under high cooling rate and pressure under quiescent conditions.[21−23]

**Experimental Procedures.** *Measurements of Spherulitic Nucleation Density and Growth Rate*. As mentioned above, in a previous work[19] some measurements of spherulitic nucleation density and growth rate during isothermal crystallization (at $T$ = 140 °C) were carried out under both quiescent and shear conditions (shear rate ranging from 0.07 $s^{-1}$ to 0.30 $s^{-1}$). In this work, a much wider set of data is obtained. In particular, measurements of spherulitic nucleation density and growth rate during isothermal crystallization were performed adopting different temperature and shear rate conditions adopting the experimental protocol already described in the previous work and summarized below.

The observation of morphology and the measurement of nucleation density and growth rate under both steady shear and quiescent conditions were performed by means of a polarized light microscope (Olympus BH-41), equipped with a shearing cell (Linkam shearing cell, CSS450). Photographs were taken by a 3CCD color video camera. The shear effect and thermal treatment were imposed by the Linkam shearing cell: steady shear was applied to the samples by rotation of the bottom quartz window at a constant angular velocity. Although the plate−plate geometry of the cell imposes different shear rates along the radial direction, shear rate was nearly constant in the observation field being the observation windows at a fixed radial position (7.5 mm in this case). The accuracy of thermal control was checked by independent tests carried out by a thermocouple. Since the imposed shear rate depends on the thickness of the sample, after any test conducted by the Linkam shearing cell the thickness of the solidified sample was accurately measured. The test was considered valid, and thus the results were analyzed, only if the measured thickness was found to be consistent with the expected thickness. Most of the experiments were conducted in duplicate, showing a good reproducibility of the results.

The isothermal crystallization of iPP resins was carried out under both quiescent and shear conditions. Polymer films with a thickness of about 200 $\mu$m were prepared, starting from pellets, by compression molding at $T$ = 210 °C. Disks were cut from these films, they were inserted into the Linkam cell, heated and melted at $T_A$ = 210 °C. Their thickness was reduced to 100 $\mu$m by slowly lowering the upper glass plate of the Linkam device. Subsequently, the sample was kept under these conditions at constant temperature for 10 min to erase previous thermal and mechanical history.

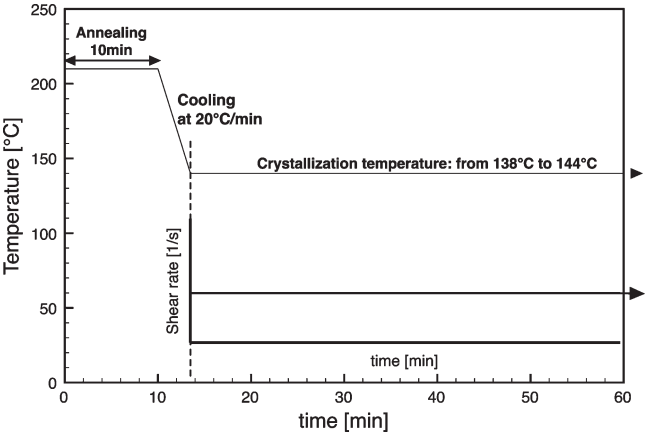


**Figure 1.** Thermo-mechanical protocol adopted for the crystallization experiments.

**Table 1. Experimental Conditions Adopted in the Crystallization Experiments in This Work**

| crystallization temperature ($T_c$) [°C] | shear rate [$s^{-1}$] |
|---|---|
| 142, 144 | 0.07 |
| 138, 139, 142, 144 | 0.11 |
| 140 | 0.125 |
| 138 | 0.175 |
| 142 | 0.15 |
| 144 | 0.15 |
| 138, 144 | 0.25 |

**Table 2. Experimental Conditions Adopted in the Crystallization Experiments in the Previous Work[19]**

| crystallization temperature ($T_c$) [°C] | shear rate [$s^{-1}$] |
|---|---|
| 140 | 0.07, 0.11, 0.15 0.175, 0.20, 0.25, 0.30 |

The microscope was focused on the central position between top and bottom windows. The temperature was then lowered at the rate of 20 °C/min until it reached the desired crystallization temperature. Zero time was assigned to the instant at which the crystallization temperature was reached. Shear flow was then applied at the chosen shear rate and images were acquired by the digital camera. The shear flow was kept constant until the crystalline structures appeared to fill most of the sample space.

Test temperatures were chosen so as to determine measurable characteristic crystallization times. In fact, too high temperatures (close to the thermodynamic melting temperature) resulted in very low crystallization rates, whereas too low temperatures caused an essentially instantaneous crystallization. In both cases, the measurements become impossible, or at best not reliable.

The thermo-mechanical protocol adopted for the crystallization experiments is described in Figure 1 and the experimental conditions are reported in Table 1 (this work) and Table 2 (the previous work[19]). In all the experimental conditions, an analysis of the significance of the viscous heating leads to the conclusion that the a negligible (less than 0.01 °C) temperature increase took place during the tests.

*Analysis of the Images*. The micrographs collected during the crystallization process taking place under shear were analyzed

by means of a software for image analysis developed at University of Salerno. Some digital filters were added to the software in order to make it more effective in identifying the elements in the micrographs. The software automatically identifies the elements in the micrographs and evaluates their number, their position and their dimension and, finally, it stores the collected information in a file.

During the crystallization process, the crystalline elements showed in the micrographs move increasing in number and dimensions as a result of the application of the shear. Therefore, the number of the nuclei could be followed and the dimension of the spherulites could be monitored as long as they remained inside the observation window that is during a time period, which depended on the test but was always longer than about 30 s. The evolution of the spherulite number and dimensions could be attained by applying the developed software for the image analysis to the series of micrographs collected during the crystallization under shear. In order to obtain reliable values of the spherulites nucleation density and growth rate a huge number of micrographs was collected during the crystallization and carefully analyzed. In particular, concerning the evolution of spherulitic radius, different spherulites were measured at different times from the beginning of the test, so that the growth rate could be measured, although on different spherulites, during the whole test time.

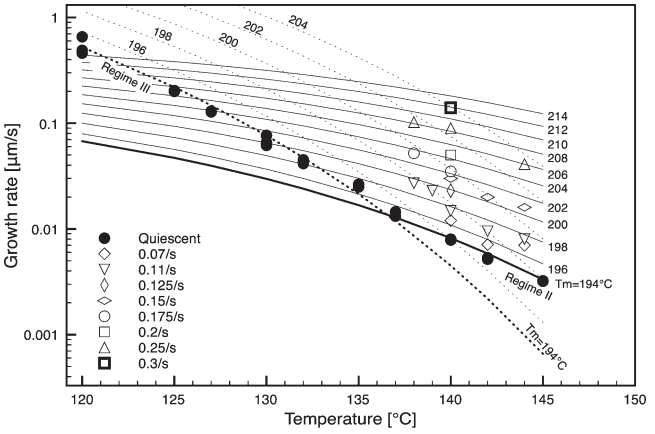


**Figure 2.** Results of growth rate in quiescent conditions (filled circles) and during shear flow (open symbols). Continuous and dotted thick lines refer to eq 1 with the parameters reported in Table 3 as "regime III" and "regime II", respectively Thinner lines are obtained by changing the only melting temperature.

## Results

**Quiescent Crystallization.** In this work, quiescent crystallization experiments were taken as a reference for all the temperatures investigated. The morphology, the nucleation density and the growth rate of the spherulites were monitored during experiments performed under quiescent conditions with the same thermal history of the shear flow experiments (Figure 1).

Nucleation density was determined by counting the number of spherulites in the sample and growth rate was determined by measuring the diameter of spherulites as a function of time until impingement took place.

Experimental determinations showed that, consistently with literature indications for the adopted material,[21] nucleation resulted to be predetermined under quiescent condition: a fixed number of nuclei appeared at the test temperature, and their number did not change in time. Furthermore, spherulite radial growth rate was found constant with time. Results of growth rate evaluated in quiescent condition are reported in Figure 2 as filled circles. In the range of temperatures investigated, growth rate decreases on increasing temperature of the isothermal test. In Figure 2, continuous and dotted thick lines were obtained by adopting different models for the description of growth rate, as described in the following Discussion.

**Crystallization under Shear Flow.** In the mentioned previous work,[19] it was found that under shear flow (shear rate ranging from 0.07 to 0.3 $s^{-1}$) at 140 °C the morphology maintained the spherulitic structure and that nucleation density increases with time whereas in quiescent conditions it remained constant and it was function only of temperature. The crystallization experiments performed in this work at 138, 139, 142, and 144 °C confirmed this behavior: in fact, the

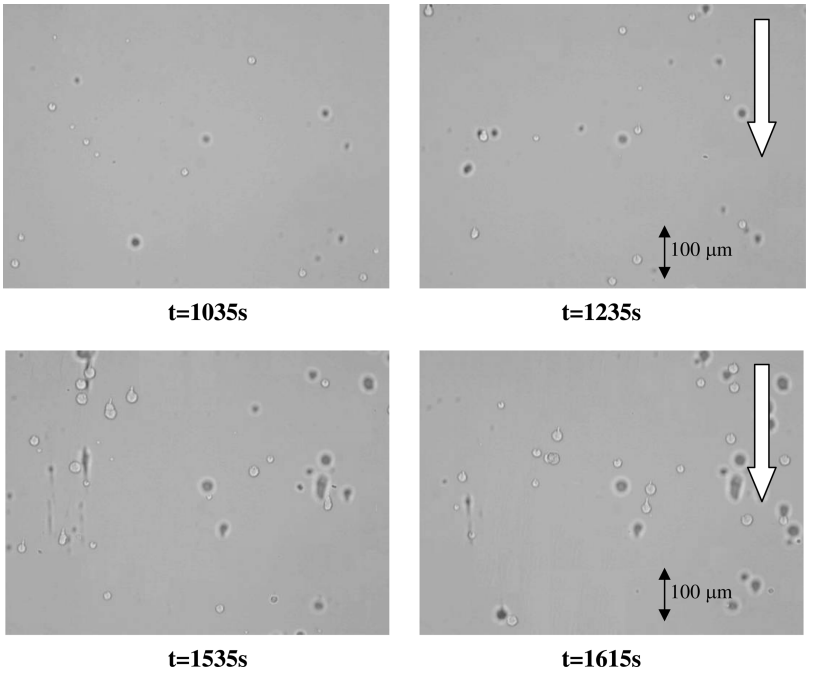


**Figure 3.** Micrographs collected during crystallization process under shear condition ($\dot{\gamma} = 0.15\ s^{-1}$ and $T = 142$ °C). Flow direction is also indicated.

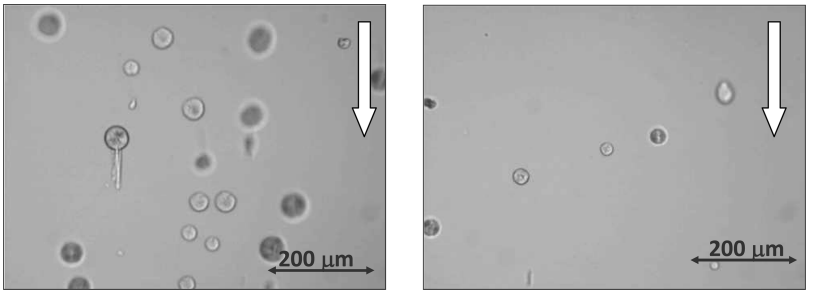


**Figure 4.** Micrographs collected during crystallization under different temperatures ($T$ = 140 (left) and 142 °C (right), $\dot{\gamma}$ = 0.07 $s^{-1}$ $t$ = 2200 s). Flow direction is also indicated in figure.

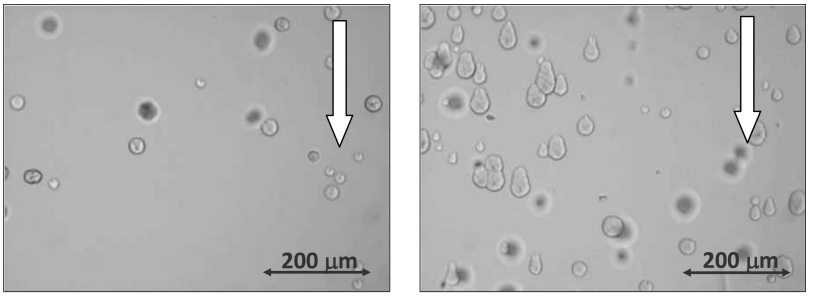


**Figure 5.** Micrographs collected during crystallization under different shear rates ((a) $\dot{\gamma}$ = 0.07 and (b) 0.15 $s^{-1}$, $t$ = 1600 s, $T$ = 140 °C). Flow direction is also indicated.

nucleation density was found to increase with time as shown in Figure 3 where micrographs collected at different times during the crystallization process under shear condition ($\dot{\gamma}$ = 0.15 $s^{-1}$ and $T$ = 142 °C) are reported. This effect is confirmed by the heterogeneity of the spherulite dimensions: in fact, the nuclei generated at different times show different dimensions.

The effects of the temperature on the morphology of the spherulitic structure are shown in Figure 4 where optical micrographs collected during crystallization under the same shear rate ($\dot{\gamma}$ = 0.07) but different temperatures (140 and 142 °C) are reported. Both of the micrographs were collected after 2200 s from the time at which temperature reached the isothermal crystallization temperature and the shear started. The figure shows that the number of nuclei strongly decreases on increasing the isothermal temperature of the test.

The effects of the intensity of the shear flow on the morphology of the spherulitic structure during crystallization at $T$ = 138 °C are shown in Figure 5 where optical micrographs collected during crystallization process under different shear rates ($\dot{\gamma}$ = 0.11 and 0.175 $s^{-1}$) are reported. Both of the micrographs were collected after 600 s from the time at which temperature reached the isothermal crystallization temperature and shear started. The figure shows that the number of nuclei after a given time strongly increases on increasing the shear rate. Concerning Figure 5b, it can be noticed that some of the crystals are elongated along the flow direction rather than being spherical. A careful observation of this phenomenon pointed out that this happens when the spherulite, while growing, interacts with the plate of the shearing cell. As mentioned above, the focus of the camera is set at the midplane of the shearing system, so that the crystals which nucleate and grow on the plates are out of focus and are not taken into consideration when measuring the nucleation density. It happens sometimes that also spherulites which nucleate far from the plates, while growing get in touch with

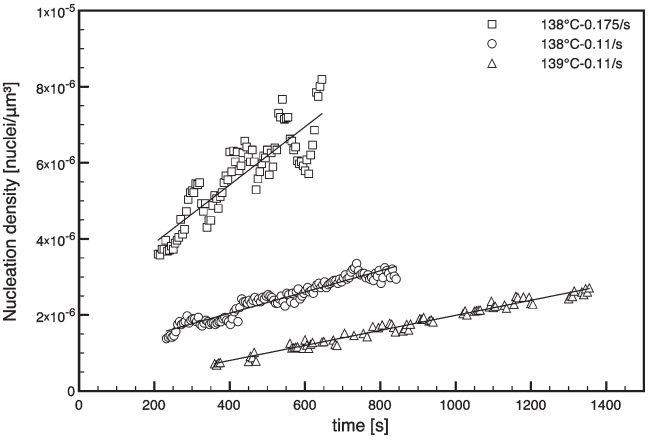


**Figure 6.** Evolution of nucleation density under steady shear flow ($T$ = 138 and 139 °C).

the plates. This causes the spherulite to elongate and grow asymmetrically (i.e., showing a tail). These crystalline entities are counted as far as the nucleation density is concerned, but are disregarded when measuring the growth rate.

*Nucleation Density Measurements*. The evolution of the nucleation density during the crystallization under shear, evaluated by means of the image analysis software, is reported in Figure 6 for the data gathered at $T$ = 138 and 139 °C and in Figure 7 for the data gathered at $T$ = 142 and 144 °C. The data reported in Figure 6 and Figure 7 confirm that at each temperature under flow conditions the number of activated nuclei strongly increases with time. Concerning the wavy behavior of some of the data set (especially those reported in Figure 6 which refer to the largest nucleation densities), it is due to the fact that, as mentioned in the Analysis of the Images section above, due to the rotation, a different region of the sample is analyzed after a time period

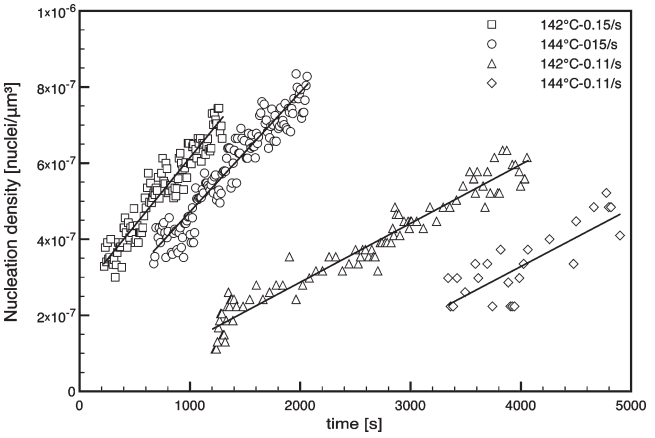


**Figure 7.** Evolution of nucleation density under steady shear flow ($T$ = 142 and 144 °C).

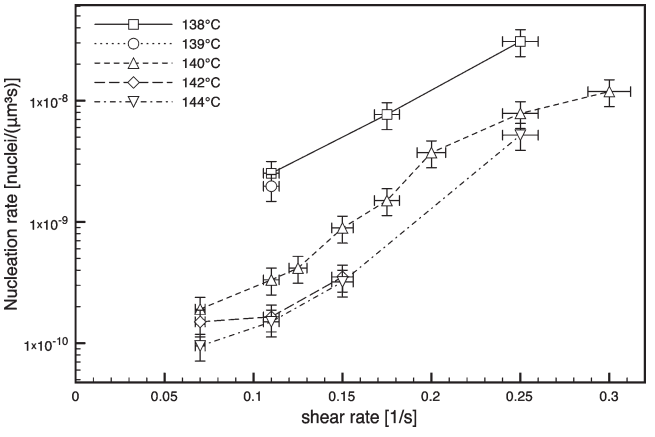


**Figure 8.** Nucleation rate obtained by a linear fitting of the evolution of nucleation density data as a function of shear rate. Data gathered in the previous work (at $T$ = 140 °C) are also reported in the figure. The shear rate error bars refer to the fact that (due to the adopted plate−plate geometry) the shear rate slightly changes along the zone considered.

which for the highest shear rates is about 30 s. Some region can be slightly richer or poorer of spherulites, and this causes an increase or a decrease of the counted number of entities.

Consistent with previous results[19] gathered at 140 °C, Figure 6 and Figure 7 show that nucleation density increases about linearly with time.

Figure 6 and Figure 7 also show the effect of temperature on the nucleation density evolution under steady shear flow for the same shear rate: the number of nuclei is larger for tests conducted with a lower temperature.

The values of nucleation rate were obtained by a linear fitting of the evolution of nucleation density for all the shear rates and temperatures applied in this work. The results are reported as a function of the shear rate in Figure 8. At each temperature, nucleation rate increases on increasing the shear rate, about linearly on a semilog scale. Furthermore, the effect of an increase of temperature at a constant shear rate is toward a reduction of the nucleation rate.

This effect is more clearly shown in Figure 9, in which the values of nucleation rate estimated in tests conducted under the same shear rate (0.11 $s^{-1}$) are reported as a function of the temperature: for temperatures ranging from 138 to 140 °C, a small decrease in the test temperature (a couple of °C) gives rise to a strong increase (1 order of magnitude) in the nucleation rate. Furthermore, Figure 9 shows that for temperature ranging from 142 to 144 °C the nucleation rate does not change significantly with temperature.

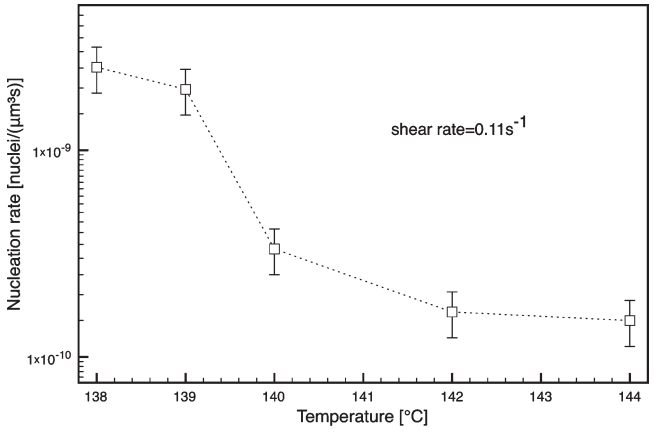


**Figure 9.** Nucleation rate obtained by a linear fitting of the evolution of nucleation density data as a function of the temperature at $\dot{\gamma}$ = 0.11/s.

*Growth Rate Measurements*. In the literature, many papers deal with the effect of shear flow on the nucleation step, and most of the authors agree on the enhancement of the nucleation rate due to the flow. In comparison, little is known about the effect of shear on the crystal growth rate, and moreover, there is not an unanimous consensus of opinion about this topic.[23−27] In our previous work,[19] measurements of crystal growth rate performed at 140 °C have shown that the growth rate is essentially constant during the test (both in quiescent and flow conditions) and that it is an increasing function of the shear rate.

During the crystallization tests under shear, if spherulites move increasing in dimensions then the spherulitic growth rate can be evaluated by monitoring their dimensions as long as they remain inside the observation window. Values of growth rate were obtained by means of the application of the software for the image analysis to the micrographs collected during the crystallization experiments. In fact, as already reported, the software for image analysis is able to identify the spherulites in the micrographs and to evaluate their dimensions. In order to evaluate the spherulitic growth rate during the shear crystallization tests, this analysis was performed on a broad number of spherulites for different crystallization times.

Values of spherulitic growth rate, obtained by a linear fitting of the evolution of spherulites dimensions for all shear rates and temperatures applied in this work, were reported as a function of the shear rate in Figure 10. The spherulitic growth rates under shear conditions are always higher than that in the quiescent state at the same temperature (Figure 2) and it is an increasing function of the shear rate. Figure 11 also shows that the effect of temperature on growth rate is quite significant: a small decrease in the test temperature gives rise to a strong increase in the spherulitic growth rate (1 order of magnitude for a decrease of few degrees Celsius). Results reported in Figures 10 and 11 give a contribution to clarify controversial effect of flow on spherulitic growth rate.

## Discussion

In the mentioned previous work,[19] it was found that, at 140 °C, nucleation rate and spherulitic growth rate are proportional. In Figure 12, growth rate measured under continuous shear is reported versus nucleation rate measured in the same conditions for all the samples analyzed. The correlation between nucleation rate and spherulitic growth rate is clearly confirmed for all the temperatures and shear rates considered. To a first approximation the growth rate is proportional to the square root of the nucleation rate.

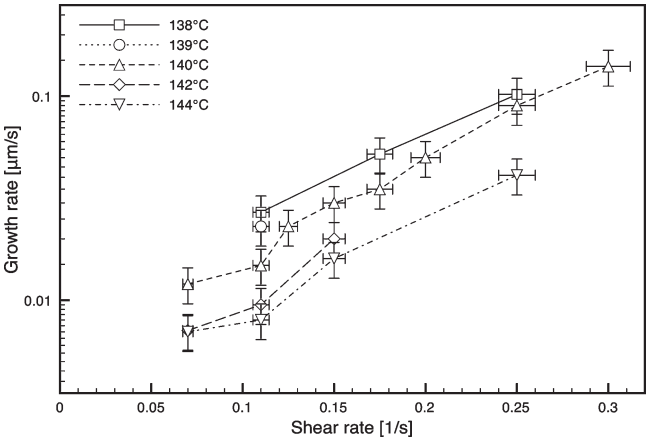


**Figure 10.** Spherulitic growth rate, obtained by a linear fitting of the evolution of spherulite dimensions for each shear rate and temperatures applied in this work, as a function of the shear rate. Experimental data gathered in the previous work[19] at $T = 140$ °C are also shown in figures. The shear rate error bars refer to the fact that (due to the adopted plate−plate geometry) the shear rate slightly changes along the zone considered.

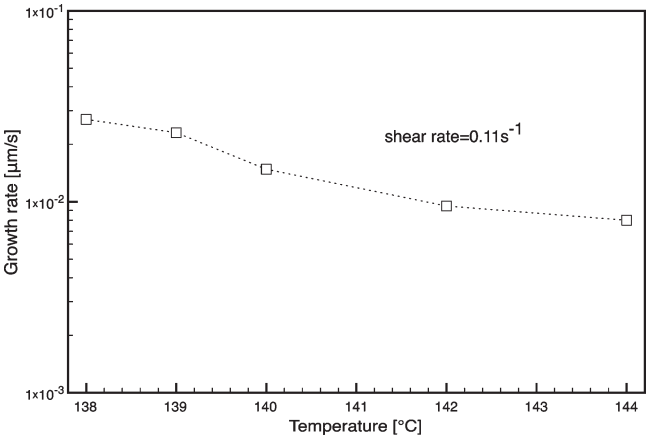


**Figure 11.** Spherulitic growth rate, obtained by a linear fitting of the evolution of spherulite dimensions for shear rate of 0.11/s as a function of the temperature.

This result suggests that, whatever the controlling mechanism for the enhancement of nucleation rate is, it has a parallel effect also on growth rate.

The idea guiding many of the papers on the effect of flow on crystallization kinetics was focused on the changes of the melting temperature due to the flow. In fact, the melting point increases because of an entropy decrease due to the flow induced chain extension in the melt and the increase in melting temperature goes together with earlier and faster crystallization.[1]

In a previous work in which quiescent conditions were cosidered,[21] the temperature dependence of the growth rate was described by identifying the parameters the following equation:[29]

$$G[T] = G_0 \exp\left[-\frac{U}{R(T-T_\infty)}\right] \exp\left[-\frac{K_g(T+T_m)}{2T^2(T_m-T)}\right] \quad (1)$$

considering a very wide set range of solidification conditions. The parameters identified in that work are reported in Table 3 (row "regime III"). It was shown that, with the found parameters, eq 1 could successfully describe data of growth rate taken at temperatures lower than 137 °C. The comparison is proposed in Figure 2, in which the filled circles represent the data of quiescent growth

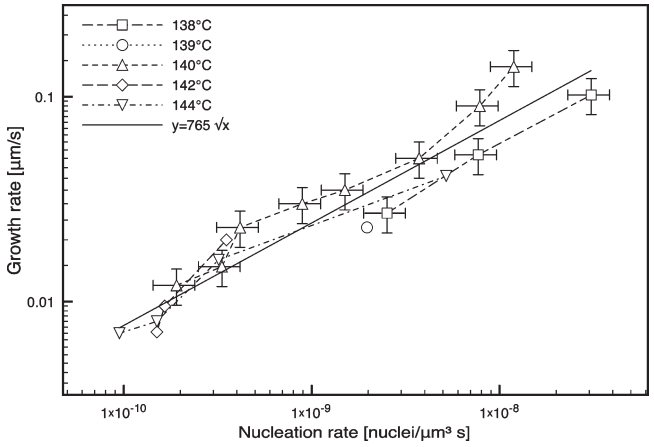


**Figure 12.** Growth rate versus nucleation rate for iPP under several temperature and shear rate conditions.

**Table 3. Values of the Parameters adopted to Describe the Experimental Data of Quiescent Spherulitic Growth Rate Measured in a Previous Work[19]**

| | $G_0$ ($\mu$m/s) | $U/R$ (K) | $K_g$ (K$^2$) | $T_\infty$ (°C) | $T_m$ (°C) |
|---|---|---|---|---|---|
| regime III | $2.9 \times 10^{10}$ | 751.6 | 534858 | −37.2 | 194 |
| regime II | $1.7 \times 10^{5}$ | 751.6 | 267429 | −37.2 | 194 |

rate and the dotted line represent the description obtained by eq 1 adopting the parameters reported in Table 3 (row "regime III").

As far as the data collected at temperatures higher than 137 °C, namely in the range of temperature of interest for this work, Figure 2 clarifies that, in the framework of the Hoffman−Lauritzen (H−L) theory, there is a change in regime at 137 °C. The H−L model assumes that at high temperatures, the advancing speed of the crystal growth front is controlled by the rate for generating a single surface nucleus (regime I). With the decrease of crystallization temperatures, multiple nucleation takes place on the substrate. This situation is termed as regime II. With further decrease of crystallization temperatures, due to the higher frequency of surface nucleation, the widths of substrates turn out to be close to the thickness of single stems; therefore, the crystallization is mainly dependent on the molecular chain transportation velocity from the melt to the crystal growth front. This condition is termed as regime III. If eq 1 is adopted to describe the growth rate, the parameters influenced by the change of regime are the prefactor $G_0$ and the nucleation constant kg. The latter term, in particular, is subject to the change among the regimes with the following ratios: $K_g(\mathrm{III}) \approx K_g(\mathrm{I}) = 2K_g(\mathrm{II})$[30]

Therefore, in order to describe the data of growth rate at temperatures higher than 137 °C, a different set of parameter must be adopted, which however requires the definition of just one free parameter, namely $G_0$, since, as specified above, $K_g$ takes a new but fixed value (one-half of the value of kg previously determined) and all the other parameters of eq 1 were left unchanged. The values of the parameters to be adopted in this work for eq 1 are reported.

Assuming that the values of the constants $G_0$, $T_\infty$, $U$, and $K_g$ do not depend on the flow conditions, once the value of $G(T)$ under flow is measured, the only unknown parameter in eq 1 is the (flow affected) melting temperature $T_m$. The increase of $T_m$ in eq 1 describes an increase of the growth rate as described in Figure 2. The values of the melting temperature for each temperature and shear rate which should be substituted in eq 1 in order to obtain the results of growth rate reported in Figure 10 are depicted in Figure 13 for all the tests conducted in this work . We considered two approaches: the first one (Figure 13a) was to keep the parameters of regime III, following the procedure reported in

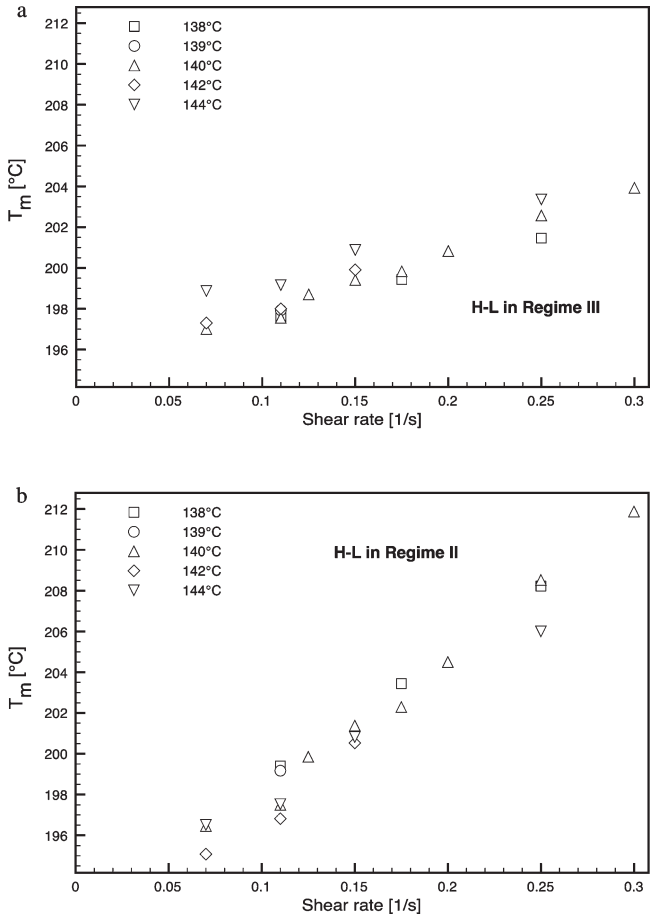


**Figure 13.** Melting temperature, $T_m$ in eq 1, as a function of shear rate (the quiescent melting temperature is estimated as $T_{mq}$ = 194 °C). (a) Results obtained by considering the H−L equation in regime III. (b) Results obtained by considering the H−L equation in regime II.

Figure 2 as dotted lines; the second one was to (Figure 13b) keep the parameters of regime II, following the procedure reported in Figure 2 as continuous lines.

Both procedures describe an increase of the melting temperature by effect of the imposed shear flow. However, the results obtained by adopting the parameters of regime III (Figure 13a) give rise to some inconsistencies: for the same shear rate, data collected at higher temperatures show larger melting temperatures. This is obviously not in line with the common understanding which would suggest for higher temperatures lower effects of the flow due to the shorter relaxation times. On the other hand, the results obtained by adopting the parameters of regime II (Figure 13b), present a similar scatter, but do not show any inconsistency. Therefore, in the following, where not explicitly mentioned, the reported flow melting temperatures are those calculated by keeping the parameters of Regime II.

The results reported in Figure 13b show that the imposed shear flow causes an increase of melting temperature as high as about 20 °C. This means that the undercooling, namely the difference between the melting temperature and the test temperature, which is a measure of the driving force of the crystallization, undergoes a significant increase under flow.

In Figure 14 (left vertical axis), the experimental values of nucleation rate are plotted versus the estimated undercooling. The temperatures at which the tests were conducted is reported close to the data.

Figure 14 shows that the correlation between the nucleation rate, obtained by a linear fitting of the evolution of nucleation density data, and the undercooling, obtained by the eq 1 according

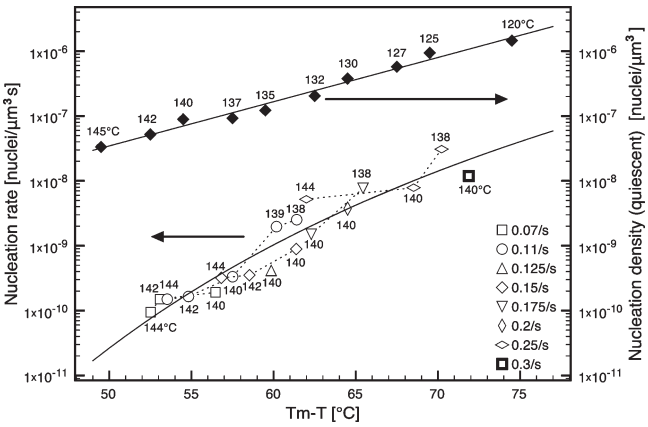


**Figure 14.** Nucleation rate, obtained by a linear fitting of the evolution of nucleation density data, analyzed in terms of undercooling (left vertical axis). The line describes an exponential dependence upon the reciprocal of the undercooling. Data of nucleation density measured during quiescent conditions are also reported (right vertical axis). For quiescent data, $T_m$ = 194 °C. The temperatures at which the tests were conducted is reported close to the data.

to the procedure shown in Figure 2, is satisfactory. In fact, results of nucleation rate, in experiments performed at temperature and shear rate substantially different, appear to be aligned; this means that the undercooling should be the parameter able to describe completely the effect of flow on nucleation rate. Figure 14 also suggests that nucleation rate, at least for the isothermal tests carried out in this work in a very wide range of conditions, is an exponential function of the undercooling or of its reciprocal (in Figure 14, the line describes an exponential dependence upon the reciprocal of the undercooling).

**Homogeneous and Heterogeneous Nucleation.** It is sometimes stated in the literature that a nucleation rate is present also under quiescent conditions:[31]

$$N(t) = \dot{N}t + N_0 \tag{2}$$

where $N(t)$ is the evolution of the total number of nuclei, $\dot{N}$ is the nucleation rate (a function of temperature and shear rate), and $N_0$ is the number of the heterogeneous nuclei generated at the chosen temperature. In a previous work,[21] the number of heterogeneous nuclei under quiescent conditions was found to depend on the temperature according to an exponential function

$$N_0(T) = \alpha \exp(\beta(T_{mq} - T)) \tag{3}$$

with $T_{mq}$ = 194 °C.

Under quiescent conditions, assuming the validity of eq 2, the time at which the continuously generated nuclei would overcome the constant number of heterogeneous nuclei can be defined as

$$t_c = \frac{N_0}{\dot{N}} \tag{4}$$

Assuming that nucleation rate is determined only by the undercooling, as shown in Figure 14, the time $t_c$ at which the continuously generated nuclei would overcome the constant number of heterogeneous nuclei, can be evaluated also under quiescent conditions. As heterogeneous nucleation density is given by eq 3 and the values of nucleation rate under quiescent conditions can be evaluated from Figure 14 at each temperature by considering the melting temperature in quiescent conditions ($T_m = T_{mq}$), the value of $t_c$ can be

calculated by eq 4 at each temperature. The results obtained would indicate for $t_c$ (under quiescent conditions) about 1000 s for an undercooling of 50 °C (namely at 144 °C), 150 s for an undercooling of 60 °C (namely at 134 °C), and 50 s for an undercooling of 70 °C (namely at 124 °C). This would mean that for all the data of nucleation density measured in quiescent conditions at these temperatures (and reported in Figure 14, right vertical axis) the phenomenon of nucleation rate should have been clearly visible, and after time periods of the order of those just specified the number of generated nuclei should have overcome the number of heterogeneous nuclei. Vice versa, according to the experimental results reported in ref 21, at 140 °C new crystallites were not observed after more than 20000 s. Thus, it is possible to conclude that under quiescent conditions nucleation rate, if present, is at least 1 order of magnitude slower than under flow, at the same undercooling. Our opinion is that nucleation rate is not present in quiescent conditions, and a threshold of shear rate exists below which the mechanism of continuous nuclei generation does not take place. This could be the same threshold for flow to affect total crystallization rate, whose existence has been recently pointed out.[32]

**The Weissenberg Number.** The next step in understanding of the fundamentals of flow-enhanced crystallization is to correlate the undercooling to a physical parameter related to the intensity of the flow, rather than to the growth rate. If the melting point increases because of an entropy decrease due to the flow induced orientation and chain extension in the melt, the purpose should be to correlate the undercooling (and thus both growth and nucleation rates) to the orientation and chain extension. In particular, the Weissenberg number, due to its definition (the dimensionless product of relaxation time and shear rate), is considered representative of the final molecular orientation in the sample, in fact, the higher is the Weissenberg number more effective is the flow in orienting the sample.

The material analyzed in this work was carefully characterized[23] according to a nonlinear dumbbell, by defining an overall relaxation time, function of shear rate, and temperature. The obtained description allows to calculate, for each of the shear tests presented in this work, a relaxation time representative of the status of the material during the test, which is determined by shear rate and temperature (the effect of crystallinity on relaxation time can be neglected due to the fact that only early stages are considered). The Weissenberg number was then calculated for each test by multiplying the shear rate by the relaxation time.

The evaluated undercooling and flow induced melting temperature are analyzed in terms of Weissenberg number and the results are reported in Figure 15. As for Figure 13, also in Figure 15 two plots are reported: the first one (Figure 15a) in which the melting temperature was calculated by considering the regime III parameters[28] of the Hoffman and Lauritzen equation; the second one (Figure 15b) in which the melting temperature was calculated by considering the regime II parameters of the same equation. The result is qualitatively similar: the melting temperature increases on increasing of the Weissenberg number and, consequently, of the molecular orientation and chain extension. However, when the parameters of regime II are adopted to calculate the melting temperature, most of the data gather on a single line. This confirms the result drawn above with reference to Figure 13 that the regime II of growth, identified for the quiescent data at $T > 137$ °C, should be considered also for the analysis of data gathered under shear conditions in the same range of temperatures. Furthermore, Figure 15b identifies in the Weissenberg number a parameter suitable to describe the effect of flow on the melting temperature and thus on growth and nucleation rates.

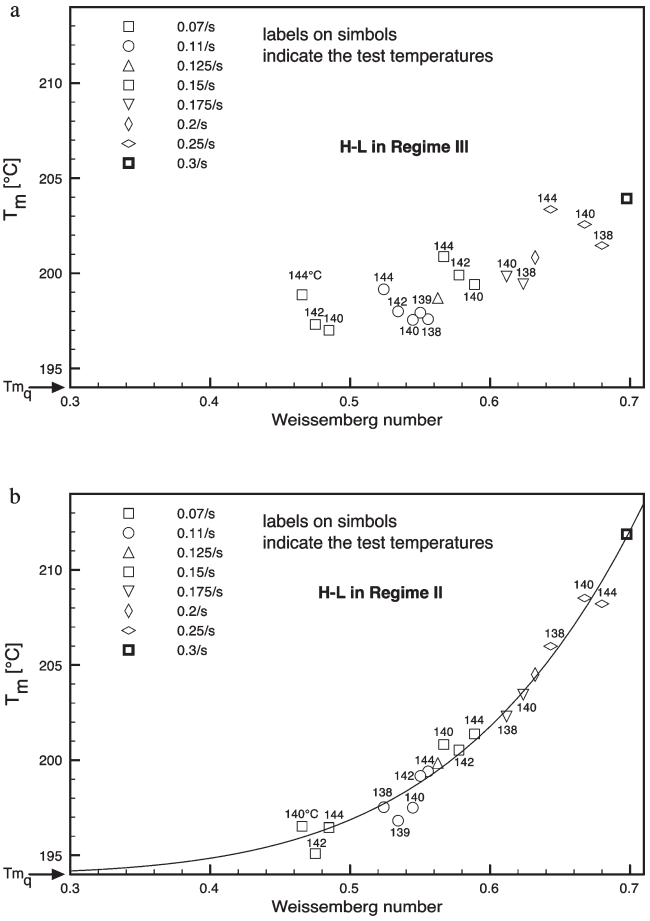


**Figure 15.** Evaluated flow induced melting temperature analyzed in terms of Weissenberg number. $T_{mq}$ is the melting temperature in quiescent conditions. (a) Results obtained by considering H−L equation in regime III. (b) Results obtained by considering H−L equation in Regime II. The line is just a guide for the eye. The temperatures at which the tests were conducted is reported close to the data.

## Conclusions

In this work, experiments on nucleation density and growth rate of spherulites were carried out under a wide range of temperature (138−144 °C) and shear rate (0−0.30 $s^{-1}$) and data of nucleation density and spherulitic radius were collected during the application of the shear.

Consistently with the results obtained in a previous work, it was found that at all temperatures, nucleation density increases about linearly with time. At each temperature, nucleation rate increases on increasing the shear rate, about linearly on a semilog scale. Furthermore, the effect of an increase of temperature at a constant shear rate is toward a reduction of the nucleation rate.

It was found that a proportionality exists between nucleation rate and spherulitic growth rate: this result suggests that, whatever the controlling mechanism for the enhancement of nucleation rate is, it has a similar effect also on growth rate.

In an attempt of identifying a parameter controlling the effect of flow on crystallization, an Hoffman−Lauritzen equation for the growth rate was assumed to be valid also under flow condition, by limiting the effect of shear rate just on the melting temperature. The other parameters were kept constant to the values determined in order to describe the quiescent data of growth rate in the same range of temperatures in which the data under flow were collected. It was also shown that, in that range, a regime II of

growth holds according to the Hoffman−Lauritzen theory and the effect of flow on the melting temperature could thus be evaluated by the experimental data of growth rate under flow conditions. The undercooling, with respect to the flow dependent melting temperature, could be thus estimated for each test, and a diagram was obtained reporting the nucleation rate versus the undercooling. It was eventually found that the nucleation rate is an exponential function of the undercooling.

In turn, the melting temperature estimated for the tests conducted in the whole range of temperatures and shear rates was found to be dependent on the Weissenberg number. With this last step, a correlation path between the Weissenberg number and both growth and nucleation rates is identified.

By analyzing the critical time at which, for a given undercooling, the number of continuously generated nuclei overcomes the constant number of heterogeneous nuclei, it was shown that under quiescent conditions nucleation rate, if present, is at least 1 order of magnitude slower than under flow, at the same undercooling. This is a clue of the fact that nucleation rate is not present in quiescent conditions, and a threshold of shear rate exists below which the mechanism of continuous nuclei generation does not take place.

## References and Notes


(1) Kumaraswamy, G.; Issaian, A. M.; Kornfield, J. A. *Macromolecules* **1999**, *32*, 7537–7547.
(2) Housmans, J.; Gahleitner, M.; Peters, G. W. M.; Meijer, H. E. H. *Polymer* **2009**, *50* (10), 2304–2319.
(3) Pennings, A. J.; Van der Mark, J. M. A. A.; Booij, H. C. *Colloid Polym. Sci.* **1970**, *236*, 99–111.
(4) Lagasse, R. R.; Maxwell, B. *Polym. Eng. Sci.* **1976**, *16*, 189.
(5) Andersen, P. G.; Carr, S. H. *Polym. Eng. Sci.* **1978**, *18*, 215.
(6) Mackley, M. R.; Keller, A. *Polymer* **1973**, *14*, 16–20.
(7) Keller, A.; Kolnaar, H. W. In *Processing of polymers*; Meijer, H. E. H., Eds.; VCH: New York, 1997; Vol. *18*, pp 189−268.
(8) Jerschow, P.; Janeschitz-Kriegl, H. *Rheol. Acta* **1996**, *35*, 127–133.
(9) Vleeshouwers, S.; Meijer, H. E. H. *Rheol. Acta* **1996**, *35*, 391–399.
(10) Pogodina, N. V.; Lavrenko, V. P.; Srinivas, S.; Winter, H. H. *Polymer* **2001**, *42*, 9031–9043.
(11) Seki, M.; Thurman, D. W.; Oberhauser, J. P.; Kornfield, A. J. *Macromolecules* **2002**, *35*, 2583–2594.
(12) Coppola, S.; Balzano, L.; Gioffredi; Maffettone, P. L.; Grizzuti, N.; Maffettone, P. *Polymer* **2004**, *45*, 3249–3256.
(13) Elmoumni, A.; Waddon, A. J.; Fruitwala, H.; Winter, H. H. *Macromolecules* **2003**, *36*, 6453–6461.
(14) Van Meerveld, J.; Peters, G. W. M.; Hütter, M. *Rheol. Acta* **2004**, *44*, 119–134.
(15) Balzano, L.; Rastogi, S.; Peters, G. W. M. *Macromolecules* **2008**, *41*, 399–408.
(16) Tribout, C.; Monasse, B.; Haudin, J. M. *Colloid Polym. Sci.* **1996**, *274*, 197–201.
(17) Li, L.; de Jeu, W. *Macromolecules* **2004**, *37*, 5646–5652.
(18) Wassner, E.; Maier, R. D. *Proc. XIII Int. Congr. Rheol.* **2000**, *1*, 183.
(19) Coccorullo, I.; Pantani, R.; Titomanlio, G. *Macromolecules* **2008**, *41*, 9214–9223.
(20) Vega, J. F.; Hristova, D. G.; Peters, G. W. M. *J. Therm. Anal. Calorim.* **2009**, *98* (3), 655–666.
(21) Coccorullo, I.; Pantani, R.; Titomanlio, G. *Polymer* **2003**, *44*, 307–318.
(22) Pantani, R.; Coccorullo, I.; Speranza, V.; Titomanlio, G. *Polymer* **2007**, *48*, 2778–2790.
(23) Pantani, R.; Coccorullo, I.; Speranza, V.; Titomanlio, G. *Prog. Polym. Sci.* **2005**, *30*, 1185–1222.
(24) Tribout, C.; Monasse, B.; Haudin, J. M. *Colloid Polym. Sci.* **1996**, *274*, 197–201.
(25) Koscher, E.; Fulchiron, R. *Polymer* **2002**, *43*, 6931–6942.
(26) Huo, H.; Meng, Y.; Li, H.; Jiang, S.; An, L. *Eur. Phys. J.* **2004**, *15*, 167–171.
(27) Tavichai, O.; Feng, L.; Kamal, M. R. *Polym. Eng. Sci.* **2006**, *46*, 1468–1475.
(28) Janeschitz-Kriegl, H.; Ratajski, E.; Stadlbauer, M. *Rheol. Acta* **2003**, *42*, 355–364.
(29) Hoffman, J. D.; Miller, R. L. *Polymer* **1997**, *38* (13), 3151–2112.
(30) Sperling, L. H., *Introduction to Physical Polymer Science*, 3rd ed.; Wiley-Interscience: New York; 2001; p 285.
(31) Naudy, S.; David, L.; Rochas, C.; Fulchiron, R. *Polymer* **2007**, *48*, 3273–3285.
(32) Ogino, Y.; Fukushima, H.; Takahashi, N.; Matsuba, G.; Nishida, K.; Kanaya, T. *Macromolecules* **2006**, *39*, 7617–7625.